

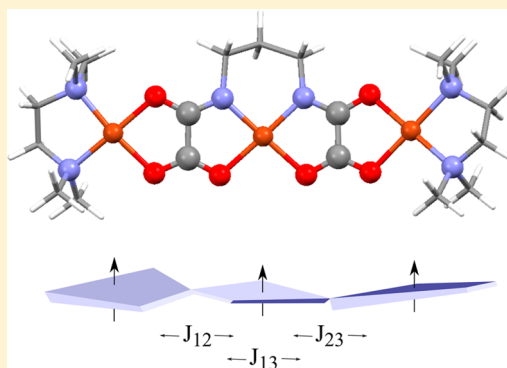
Handling Magnetic Coupling in Trinuclear Cu(II) Complexes

Daniel Reta Mañeru,[†] Ramon Costa,[‡] Meritxell Guix Márquez,[‡] Ibério de P. R. Moreira,[†] and Francesc Illas^{*,†}

[†]Departament de Química Física & Institut de Química Teòrica i Computacional (IQTCUB), Universitat de Barcelona, C/Martí i Franquès 1, 08028 Barcelona, Spain

[‡]Departament de Química Inorgànica & Institut de Química Teòrica i Computacional (IQTCUB), Universitat de Barcelona, C/Martí i Franquès 1, 08028 Barcelona, Spain

ABSTRACT: The problem of deriving three different two-body magnetic couplings in three electrons/three centers in a general geometric arrangement is investigated using the trinuclear Cu(II) HAKKEJ complex as a real case example. In these systems, one quartet and two doublet low lying electronic states exist, which define the magnetic spectra. However, the two possible linearly independent energy differences do not provide enough information to extract the three magnetic coupling constants. Here, we show how to obtain these parameters without making any assumption on the symmetry of the system from a combination of density functional- and wave function-based calculations. The density functional calculations explore various broken symmetry solutions and relate the corresponding energy to the expectation value of the Heisenberg Hamiltonian. This allows one to obtain all magnetic couplings, although their magnitude strongly depends on the exchange–correlation functional. Interestingly, a constant ratio between the magnetic coupling constants along a series of investigated functionals is found. This provides an additional equation to be used when relying on energy differences between spin states, which in turn allow solving the Heisenberg spectrum. The magnetic couplings thus obtained are compared to the experiment. Implications for the appropriate interpretation of the experiment and for the study of more complex systems are discussed.



1. INTRODUCTION

The theoretical study of magnetic interactions on transition metal complexes has deserved copious attention during the past decades.^{1–5} The crucial goals have been to understand the dependence of the magnetic properties on the structural parameters and the accurate prediction of the magnetic coupling constants. These are not simple tasks due to the complex nature of the magnetic interactions involving electronic states in a very narrow range of energy. Nevertheless, the investigation of the magnetic coupling mechanism in terms of electronic interactions^{3–5} provides the way to analyze the magnetic properties and their structural correlations. These constitute valuable and useful tools to design novel molecular and extended magnetic materials with potential technological applications.

The relative simplicity and wide structural diversity of Cu(II) dinuclear complexes makes them ideal systems for the study of magnetic properties either from experiment¹ or theory.^{3–5} Not surprisingly, the structural and magnetic properties and the details of their electronic structure have been determined in detail. It is nowadays well established that these systems can be described in terms of a Heisenberg (more properly Heisenberg–Dirac–Van Vleck or HDVV) Hamiltonian with one $S = 1/2$ spin moment per Cu(II) center. It is important to point out that the spin moments arise from the d^9 electronic configuration of the Cu(II) center. Hence, there is one electron

per magnetic center strongly localized on a single atomic-like magnetic molecular orbital. However, the coordination around the magnetic center quenches the orbital angular momentum and, consequently, spin–orbit effects can be neglected. The two $S = 1/2$ spin moments couple in one triplet (T with total magnetic spin $S = 1$) and one singlet (S with total magnetic spin $S = 0$) states. The ordering and energy separation between these two spin states determine the sign and magnitude of the exchange coupling constant J defining the Heisenberg Hamiltonian. The magnitude of the J value can be extracted from experimental data concerning magnetic susceptibility versus temperature and making use of the Bleaney–Bowers equation⁶ relating the product of the molar susceptibility and temperature ($\chi_M T$) to temperature. Alternatively, J can be predicted from theoretical calculations as the energy difference between the two low-lying triplet and singlet spin states. This is the basis of the mapping procedure as described in detail in the review paper by some of us.⁴

Due to the special features of dinuclear copper(II) complexes commented on above, these systems have been extensively studied by means of *ab initio* methods, either from accurate wave function-based methods^{7–10} or advanced density functionals^{11–15} and provide a convenient open-shell database¹³ to

Received: May 20, 2015

check the accuracy of further developments. The former allow for a deep understanding of the physical mechanisms behind magnetic coupling^{5,16–18} whereas the latter open the door to the study of magnetic coupling in larger systems.¹⁹ For these homodinuclear complexes and as a result of these efforts, the extraction of the magnetic coupling constants by means of wave function and/or density functional theory (DFT)-based methods, together with the appropriate mapping are well defined and established.^{12,20} The mapping approach has also been recently used to investigate magnetic coupling in a variety of heterodinuclear complexes.²¹

Unfortunately, the usual mapping approach may fail when considering systems involving more than two magnetic centers. More specifically, the mapping approach cannot be applied when the number of pure spin states—eigenfunctions of the square of the total spin operator and of its *z*-component—leads to a number of linear independent energy differences smaller than the number of two-body magnetic couplings. This limitation comes from the specific nature of the system of interest and even knowing the exact solution, either via wave function-based methods or through the exact universal functional will not provide a solution, and other alternative approaches are needed as discussed below. Let us simply consider the case of a trinuclear Cu(II) complex. Following the line of reasoning described above, there are three $S = 1/2$ spin moments well localized in each center and coupled to two doublet (D_1 and D_2) and one quartet (Q) states. For a trinuclear complex, the most general form of the Heisenberg Hamiltonian with two-body interactions only involves three magnetic coupling constants (J_{12} , J_{13} , and J_{23} , where 1, 2, and 3 correspond to each magnetic center in a 1–2–3 topology). The three electronic states lead to two linear independent equations regarding the energy difference involving the D_1 , D_2 , and Q electronic states. Therefore, from the low lying energy spectrum, it is not possible to determine the three magnetic coupling constants. This problem also affects the fitting of experimental data, which requires some initial physically meaningful guess and depending on the particular choice, it is possible to come out with different sets of coupling constants that equally represent the experimental magnetic susceptibility versus temperature curve. To avoid this problem it is customary to neglect some of the terms or to rely on symmetry. In the case of strictly symmetric systems in which a symmetry element relates two of the magnetic centers (1 and 3) and passes across the third one (2), one can safely state that $J_{12} = J_{23} = J$ with a concomitant simplification of the spectrum arising from the corresponding Heisenberg. In this case, the energy spectrum becomes much simpler. Assuming an antiferromagnetic D_1 ground state where energy is arbitrarily set to zero, the energy of D_2 is $-J/J_{13}$ and that of Q is $-3J/2$. In this case, the two magnetic coupling constants of interest are again determined univocally from energy differences. The recently reported two trinuclear linear complexes $[\text{Cu}(\text{II})_3(\text{L})_2](\text{BF}_4)_2$ and $[\text{Ni}(\text{II})_3(\text{L})_2(\text{MeOH})_4](\text{BF}_4)_2$ supported by the L^{2-} multidentate ligand derived from $\text{H}_2\text{L} = 5,5'$ -pyridyl-3,3'-bi-1H-pyrazole constitute paradigmatic examples of real centrosymmetric systems.²² For pseudosymmetric systems, the common approach used by magnetochemists to derive the magnetic couplings from the magnetic susceptibility versus temperature curves is simply to ignore deviations from symmetry. Often, a further simplification is added for linear systems where terminal centers 1 and 3 are far enough and not directly connected by any bridging ligand, which consist simply in neglecting J_{13} even

if there is no physical justification. Although these simplifications facilitate the fitting procedure and give an accurate enough estimate of the sign and magnitude of the most intense coupling constants, the information regarding to which extent the $J_{12} = J_{23}$ and $J_{13} = 0$ hypothesis hold is lost.

In the case of the theoretical prediction of magnetic coupling constants, a general and elegant alternative to the use of symmetry constraints consists in the *ab initio* derivation of the effective spin Hamiltonian and to extract the coupling constants from the pertinent matrix elements. Effective Hamiltonians provide a powerful tool described in detail in the review paper of Malrieu et al.⁵ and is used, among other applications, to derive the magnetic coupling constants in systems with two unpaired electrons per magnetic site.²³ The derivation of effective Hamiltonians in more complicated cases has been recently reported from spin-flip methods.²⁴ This procedure also allows one to recover pure spin states, but again, in the present case the information arising from the pure spin states is insufficient to determine the three coupling constants. Nevertheless, the derivation of the effective Hamiltonian is far from being routine; it requires obtaining complex matrix elements and a general computer code does not yet exist. In the present paper, we use a theoretical approach that combines wave function- and DFT-based calculations; the latter exploits the existence of many broken symmetry solution and is based in the seminal work of Noodleman aimed to extract two-body magnetic constants in a number of transition metal dimers.^{25–27} However, the present strategy involves a subtle difference. In the original work of Noodleman,²⁵ and in most of the subsequent applications (see refs 2–4 and references therein), the idea is to approximate the energy of the pure spin states from the energy of the broken symmetry solutions by appropriate spin projection. This is the case even in complex systems such as those involving several magnetic centers as in tetranuclear iron–sulfur clusters²⁸ and also applies to the spin-flip techniques commented on above.²⁴ Here, following a proposal by some of us,⁴ we will make use directly of the energy of the broken symmetry solutions—without spin projection—and appropriately map them into the expectation value of the energy of the corresponding broken symmetry solutions of the HDVV Hamiltonian. To illustrate the overall procedure while preserving the simplicity as much as possible, we have chosen to study a linear trinuclear pseudosymmetric system, whose structure consists of a central Cu(II) ion coordinated to two identical bridging ligands that connect it to two equal Cu(II)-terminal ligand fragments as described in detail in Section 3.

2. RECOVERING THE HEISENBERG PICTURE FROM BROKEN SYMMETRY SOLUTIONS

To illustrate the main ideas behind the mapping approach used in the present work, we recall that for a system with three $S = 1/2$ magnetic centers in a 1–2–3 asymmetrical topology, the low energy spectrum is well described by a HDVV Hamiltonian.

$$\begin{aligned}\hat{H}^{\text{HDVV}} &= - \sum_{\langle i,j \rangle} J_{ij} \cdot \hat{\mathbf{S}}_i \cdot \hat{\mathbf{S}}_j \\ &= -J_{12} \cdot \hat{\mathbf{S}}_1 \cdot \hat{\mathbf{S}}_2 - J_{23} \cdot \hat{\mathbf{S}}_2 \cdot \hat{\mathbf{S}}_3 - J_{13} \cdot \hat{\mathbf{S}}_1 \cdot \hat{\mathbf{S}}_3\end{aligned}\quad (1)$$

In the most general case, this spectrum involves the D_1 , D_2 , and Q states described in the Introduction. These states can be expressed as a linear combination of the $|\alpha\alpha\beta\rangle$, $|\alpha\beta\alpha\rangle$, and $|\beta\alpha\alpha\rangle$ basis set elements, which are eigenfunctions of the *z*-

component of the total spin; the +1/2 component is chosen for convenience. By diagonalizing the matrix representation of the HDVV Hamiltonian in the above-mentioned basis set, one obtains,²⁹

$$|D_1\rangle = 2^{-1/2}(|\alpha\alpha\beta\rangle - |\alpha\beta\alpha\rangle) \quad (2)$$

$$|D_2\rangle = 6^{-1/2}(|\alpha\alpha\beta\rangle + |\alpha\beta\alpha\rangle - 2\cdot|\beta\alpha\alpha\rangle) \quad (3)$$

$$|Q\rangle = 3^{-1/2}(|\alpha\alpha\beta\rangle + |\alpha\beta\alpha\rangle + |\beta\alpha\alpha\rangle) \quad (4)$$

and the corresponding eigenvalues are

$$E_{D_1} = 1/4 \cdot (J_{12} + J_{13} + J_{23}) - 1/2 \cdot X \quad (5)$$

$$E_{D_2} = 1/4 \cdot (J_{12} + J_{13} + J_{23}) + 1/2 \cdot X \quad (6)$$

$$E_Q = -1/4 \cdot (J_{12} + J_{13} + J_{23}) \quad (7)$$

with

$$X = (J_{12}^2 + J_{13}^2 + J_{23}^2 - J_{12} \cdot J_{13} - J_{12} \cdot J_{23} - J_{13} \cdot J_{23})^{1/2} \quad (8)$$

from which the following expressions for the energy differences are obtained.

$$E_Q - E_{D_1} = 1/2 \cdot (-J_{12} + J_{13} + J_{23}) + X \quad (9)$$

$$E_Q - E_{D_2} = 1/2 \cdot (-J_{12} + J_{13} + J_{23}) - X \quad (10)$$

Note that these expressions, derived from the original work by Sinn,²⁹ hold in the case that the low-spin eigenstates are the ground states. For a system with the quartet state as the ground state, one would simply have

$$E_Q - E_{D_1} = 1/2 \cdot (-J_{12} + J_{13} + J_{23}) - X \quad (9')$$

$$E_Q - E_{D_2} = 1/2 \cdot (-J_{12} + J_{13} + J_{23}) + X \quad (10')$$

In the absence of further assumptions, these equations do not provide enough information to extract the three magnetic coupling constants. Note in passing by that the exact and HDVV Hamiltonians both commute with the square of the total spin and, obviously, with the z-component of the total spin operators. Hence, the eigenfunction in eqs 2–4 are spin eigenfunctions. The exact solutions are also spin eigenfunctions, and there is a one to one correspondence between these two sets. References 4 and 20 show examples of the application of the mapping approach issued from the original works of Noodleman^{25–28} to binuclear complexes and applied here to the case of trinuclear systems. The mapping is clearly illustrated in Figure 1 and, in the present case, evidence that it does not allow one to extract the three magnetic coupling constants from energy differences involving pure spin states only (see also eqs 9 and 10).

Let us now consider the Ising Hamiltonian involving only the z-component of the spin operators in eq 1

$$\begin{aligned} \hat{H}^{\text{Ising}} &= - \sum_{\langle i,j \rangle} J_{ij} \cdot \hat{S}_i^z \cdot \hat{S}_j^z \\ &= -J_{12} \cdot \hat{S}_1^z \cdot \hat{S}_2^z - J_{23} \cdot \hat{S}_2^z \cdot \hat{S}_3^z - J_{13} \cdot \hat{S}_1^z \cdot \hat{S}_3^z \end{aligned} \quad (11)$$

It is easy to show that $|\alpha\alpha\beta\rangle$, $|\alpha\beta\alpha\rangle$, and $|\beta\alpha\alpha\rangle$ basis set elements used to represent the HDVV eigenfunctions are already eigenfunctions of the Ising Hamiltonian; the corresponding values are given in eqs 12–14.

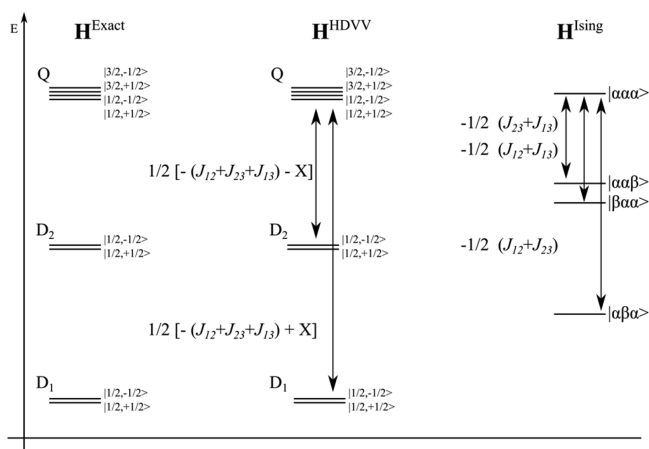


Figure 1. Schematic representation of the low lying spectrum of the exact, HDVV, and Ising Hamiltonians with X defined in eq 8. Note that in the case of the exact and HDVV Hamiltonians, the corresponding eigenfunctions (cf. eqs 2–4) are also spin eigenfunctions. Note that $X = (J_{12}^2 + J_{13}^2 + J_{23}^2 - J_{12} \cdot J_{13} - J_{12} \cdot J_{23} - J_{13} \cdot J_{23})^{1/2}$ as in eq 8.

$$E_{\alpha\alpha\beta}^{\text{Ising}} = 1/4 \cdot (-J_{12} + J_{13} + J_{23}) \quad (12)$$

$$E_{\alpha\beta\alpha}^{\text{Ising}} = 1/4 \cdot (J_{12} - J_{13} + J_{23}) \quad (13)$$

$$E_{\beta\alpha\alpha}^{\text{Ising}} = 1/4 \cdot (J_{12} + J_{13} - J_{23}) \quad (14)$$

For completeness, it is convenient to consider also the high $|\alpha\alpha\alpha\rangle$ spin function, which in this case is also eigenfunction of the HDVV Hamiltonian, and the eigenvalues for HDVV and Ising Hamiltonians coincide.

$$E_{\alpha\alpha\alpha}^{\text{Ising}} = -1/4 \cdot (J_{12} + J_{13} + J_{23}) = E_Q \quad (15)$$

The same result is obviously obtained if one uses the appropriate combination of the $|\alpha\alpha\beta\rangle$, $|\alpha\beta\alpha\rangle$, and $|\beta\alpha\alpha\rangle$ basis set elements given in eq 4, which corresponds to the $M_S = 1/2$ component of the Q spin state. Interestingly, with the $|\alpha\alpha\beta\rangle$, $|\alpha\beta\alpha\rangle$, and $|\beta\alpha\alpha\rangle$ basis set elements, the Ising Hamiltonian has four eigenvalues, four energy levels (Figure 1) and, consequently, three energy differences, which would allow one to extract the three Ising magnetic coupling constants of interest.

$$E_{\alpha\alpha\alpha}^{\text{Ising}} - E_{\alpha\alpha\beta}^{\text{Ising}} = -1/2 \cdot (J_{13} + J_{23}) \quad (16)$$

$$E_{\alpha\alpha\alpha}^{\text{Ising}} - E_{\alpha\beta\alpha}^{\text{Ising}} = -1/2 \cdot (J_{12} + J_{23}) \quad (17)$$

$$E_{\alpha\alpha\alpha}^{\text{Ising}} - E_{\beta\alpha\alpha}^{\text{Ising}} = -1/2 \cdot (J_{12} + J_{13}) \quad (18)$$

Note also that by combining appropriately eqs 16–18, one gets

$$\begin{aligned} (E_{\alpha\alpha\alpha}^{\text{Ising}} - E_{\alpha\alpha\beta}^{\text{Ising}}) - (E_{\alpha\alpha\alpha}^{\text{Ising}} - E_{\alpha\beta\alpha}^{\text{Ising}}) + (E_{\alpha\alpha\alpha}^{\text{Ising}} - E_{\beta\alpha\alpha}^{\text{Ising}}) \\ = -J_{13} \end{aligned} \quad (19)$$

One may properly argue that the coupling constants thus determined are those of the Ising Hamiltonian and hence do not represent the real system, which is described through the HDVV Hamiltonian. At this point, one must realize that the eigenvalues of the Ising Hamiltonian in eqs 12–15 coincide with the diagonal elements of the matrix representation of the HDVV in the same basis set. Since there is a one to one

correspondence between eigenvalues of the exact and HDVV Hamiltonians (Figure 1), one can safely take the energy expectation value of the exact Hamiltonian within this basis set and make use of the relationships in eqs 16–19. This would require variationally minimizing these energy expectation values, which can be done with an appropriate quantum chemical method. Since, in practice, the basis set elements correspond to single Slater determinants of the broken symmetry type, one can for instance choose an appropriate DFT method. This is not free of problems since magnetic coupling constants computed within the broken symmetry approach and DFT methods are known to strongly depend on the particular choice of the exchange correlation potential.^{12–15,30,31} To overcome this difficulty, we suggest one obtains the three coupling constants with a variety of functionals. We will show that while the absolute value of the magnetic coupling constants largely depends on the functional used, the relative values J_{23}/J_{12} and J_{13}/J_{12} are almost constant. Next, one can plug the magnetic coupling constants relationships in the HDVV Hamiltonian spectrum and simplify the expressions of the energetic differences between spin-adapted states, which in turn can be obtained from accurate ab initio wave function-based calculations. In addition, if both relationships are used, the consistency of the overall procedure can be checked because both $E_Q - E_{D_1}$ and $E_Q - E_{D_2}$ in eqs 9 and 10 will depend only on one parameter (i.e., J_{12}). Since the precise numerical value of $E_Q - E_{D_1}$ and $E_Q - E_{D_2}$ is obtained from ab initio calculations, there will be two different estimates of $E_Q - E_{D_1}$ and $E_Q - E_{D_2}$, and in the case of coincidence, one will have confirmed the validity of the present approach. A further check is provided by comparison to available experimental data.

Therefore, the combination of wave function-based methods and of DFT calculations within the broken symmetry approach opens the door to recover the simplicity of the mapping procedure. Note, however, that this mapping does not intend to recover the energy of the pure spin states. It only attempts to provide additional information to extract the full set of magnetic coupling constants from first-principles arguments. The feasibility of the present approach will be further verified by numerical calculations on a real trinuclear linear and no symmetrical Cu(II) system for which experimental values are available, as described in the forthcoming sections.

3. DEFINING A CONVENIENT TEST SYSTEM

To test the feasibility and accuracy of the mapping procedure described in the previous section, we have searched the Cambridge Structural Database (CCDC) for an appropriate linear trinuclear pseudosymmetric system. The structure chosen is derived from the HAKKEJ³² one in the CCDC; it consists of a central Cu(II) ion coordinated to two identical oxamato bridging units, which is able to transmit moderate antiferromagnetic interactions, connecting two additional Cu(II) ions with terminal ligand fragments. This structure fulfills the requirements that all atoms, included hydrogen, are well defined with an occupancy factor of 1 and that the counterions or water molecules are far enough from the magnetic centers to not affect the magnetic exchange.

The crystal structure of HAKKEJ, represented in Figure 2a, contains a trinuclear core with the central Cu(2) atom coordinated by a ligand formed by two oxamato bridges held together by a propylene chain. The metal ion lies in an almost square-planar environment with a slight tetrahedral distortion.

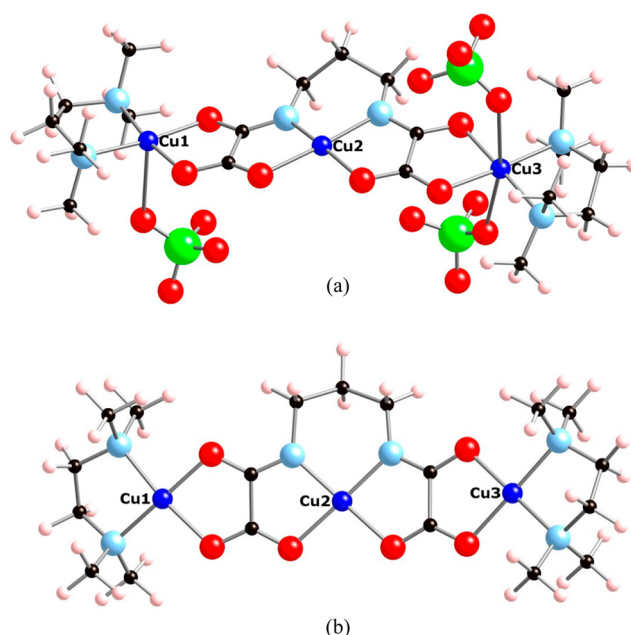


Figure 2. Molecular structure of HAKKEJ (a) and of the reduced model used in the calculations neglecting the perchlorate counterions (b).

The terminal copper atoms are blocked against polymerization by the quelling amine *N,N,N',N'*-tetramethylethylenediamine (tmen) and linked to the central core through the bridging oxamato residues. The Cu(1) ion has a 4 + 1 coordination, the basal plane being formed by the two nitrogen atoms from the amine and the two oxygen atoms from the oxamate. The Cu(1) coordination is completed by the apical oxygen atom O(9) from the perchlorate(1) anion at 2.723 Å. Cu(3) lies in a 4 + 2 coordination environment, with a basal plane similar to that described for Cu(1) with the axial positions occupied by the oxygen atoms O(7) and O(11) of perchlorate anions (1) and (2) at 2.587 and 2.875 Å, respectively. Note also that while, for convenience, the structure depicted in Figure 2a contains three perchlorate anions, the full crystallographic unit cell involves only two; the third one is, in fact, connected to another periodically repeated trinuclear unit. Since the distance from the metal center to the perchlorates is long and the Cu(1) and Cu(3) ions deviate less than 0.11 Å from the mean basal planes, all the magnetic orbitals must be strongly localized inside the copper basal planes. It is thus reasonable to neglect the perchlorate anions when attempting to compute the magnetic states of interest. Therefore, all calculations have been carried out using the resulting trinuclear dicationic fragment in Figure 2b.

In order to compare calculated results to the experiment, it is worth mentioning that the magnetic coupling constant of HAKKEJ was obtained from susceptibility (χ) measurements in the 4.2–300 K range. The experimental data were converted to $\chi_m T$ versus T plots and fitted assuming the Van Vleck expression for the simplified symmetric spin Hamiltonian $H = -J(S_1 S_2 + S_2 S_3)$ and including a Curie–Weiss parameter to take into account the weak intermolecular interactions. The least-squares regression value found for the compound was -379 cm^{-1} . Note that J_{13} has been neglected in the fitting.

An important feature of the model systems chosen in this work is that it can be artificially fragmented into two dinuclear species for which the calculation of the magnetic coupling

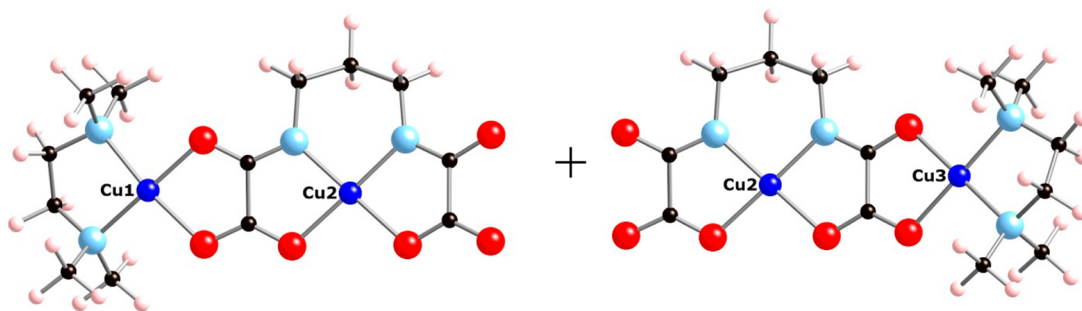


Figure 3. Two model dinuclear neutral molecules constructed from the entire HAKKEJ structure.

constant is more straightforward. The idea behind these new models is to check how similar/different the magnetic coupling constants are and to unequivocally assign the two central-terminal coupling constants J_{12} and J_{23} to the correct magnetic centers. This will provide a rough indirect estimate of the magnetic asymmetry in the trinuclear complex, an important piece of information required to carry out the fitting to experimental data and also regarding the locality of the magnetic interaction. These values will also be compared to those obtained from the general mapping procedure and to the experimental value obtained as indicated above. In order to both obtain suitable dinuclear species that can exist independently while keeping the coordination sphere of the central Cu(II) ion, the fragments have been built preserving the integrity of the whole bridging ligand with appropriate charge compensation. The two artificial neutral moieties thus constructed are described in Figure 3. At first sight, these two dinuclear model systems look very similar. However, a close examination of the distances and angles reveals non-negligible differences, which are consistent with the pseudosymmetric structure of HAKKEJ.³² It is worth pointing out that these hypothetical complexes closely resemble those experimentally described by Ribas et al.³³

4. COMPUTATIONAL DETAILS

Calculations for the trinuclear model system in Figure 2b have been carried out using a variety of wave function- and DFT-based methods. For simplicity and to avoid complications arising from different atomic structures, all calculations have been carried out using the crystallographic coordinates and with a total charge of +2 to compensate the removing of the perchlorate counteranions.

The DFT calculations have been carried out with the Gaussian 09 suite of programs.³⁴ Following previous work on dinuclear complexes, the DFT calculations have been performed using the BHandHLYP³⁵ and the popular B3LYP³⁶ hybrid functionals, the M06 and M062X hybrid meta-GGA developed by Zhao and Truhlar,^{37–39} and the range separated functionals proposed by Scuseria and collaborators; in particular, we used the HSE06 (HSEh1PBE keyword in Gaussian 09) short-range^{40,41} and the LC- ω PBE long-range⁴² corrected. Note that the selected functionals incorporate different amounts of Fock exchange: 20% for B3LYP, 27% for M06, 50% for BHandHLYP, and 54% for M06-2X. All calculations were carried out within the unrestricted Kohn–Sham formalism and the use of broken symmetry solutions, except for the highest multiplicity. The energy values thus computed have been used to estimate the magnetic coupling constants through eqs 16–18.

For the wave function-based calculations, we used a variety of methods of increasing accuracy, starting with the CASSCF(3,3) wave function⁴³ as a reference to second order perturbation, introduced either variationally, through multireference configuration interaction (MRCI) calculations using the Difference Dedicated Configuration Interaction (DDCI)⁴⁴ or perturbatively. In the last case, second-order perturbation was obtained through the well-known CASPT2^{45–47} procedure as well as through Multi Reference Møller–Pleset (MRMP).^{48–51} Note that MRMP is sometimes denoted as MCQDPT for Multi-configurational Quasi Degenerate Perturbation Theory. Both MRMP and CASPT2 use the CASSCF wave function as starting zeroth order description. The wave function-based calculations were carried out using the MOLCAS7.6 package,⁵² which was also interfaced with the CASDI⁵³ code for the DDCI calculations. MRMP on top of CASSCF calculations were carried out using the GAMESS13 code.^{54,55} It is worth mentioning that the difference between CASPT2 and MRMP perturbation theories lies in the states used to span the first-order wave function. In CASPT2, single and double excitations are applied to the reference wave CASSCF function, while in MRMP, all singly and doubly excited determinants obtained from each of the determinants in the reference wave function are considered. In other words, CASPT2 uses a contracted reference function, whereas MRMP does not. We have carried out these two types of calculations because of the nature of the doublet states here treated, as explained in the forthcoming section. Finally, it is worth pointing out that in order to make the calculations feasible the DDCI values have been carried out considering a subset of orbitals either in the occupied and virtual subspaces chosen from the CASSCF(3,3) solution for the quintet state. Hence, by freezing 70 doubly occupied and deleting 250 virtual orbitals, 187 electrons have been explicitly correlated using 377 orbitals; with these setting the number of determinants included in the DDCI expansion rises to 1.9×10^8 , this is quite at the limit of present computational resources. The same expansion was used to determine the energy of the Q , D_1 , and D_2 states.

The basis set used for all DFT, CASPT2, and DDCI calculations is the standard 6-311G⁵⁶ extended with an f function with exponent of 0.528 for Cu, the 6-31G(p,d)⁵⁷ for the H, C, N, and O atoms. For the MRMP calculations, it has been necessary to use a slightly reduced basis set for Cu and H. Thus, the H atoms are described with the 6-31G basis set, and the [Ar]-cores of Cu atoms have been substituted by the LANL2 effective core potential and the valence electrons described with the LANL2DZ basis set^{58–60} extended with an f function with exponent of 0.528.

5. NUMERICAL VALIDATION AND DISCUSSION

Let us start by analyzing the hypothetical Cu-dinuclear models. In all calculations, the magnetic interaction between the neighboring Cu(II) ions through the oxamato bridge is predicted to be antiferromagnetic, in agreement with the experiment. However, the J values calculated using the broken symmetry approach appear to exaggeratedly depend on the exchange–correlation potential with values ranging from -258 and -243 cm^{-1} , respectively, at the BHandHLYP level to -2629 and -2359 cm^{-1} , respectively, as predicted by the B3LYP method. In both cases, the calculated values are far from being identical, thus providing a first indication that the J_{12} and J_{23} of the real HAKKEJ trinuclear complex are likely to be similar but also noticeably different. However, the difference between the values predicted by the different methods is clearly too large, much larger than encountered for similar dinuclear complexes,^{4,12,13,15} which hinders making use of these results to reach reliable conclusions. A close inspection of the dinuclear models evidence that the neglect of the third Cu(II) magnetic center may induce artifacts in the electronic distribution of the resulting fragments. In order to investigate whether this is the case, a new series of calculations have been launched in which the presence of the third Cu(II) is modeled through a total ion potential (TIP) consisting of a +2 charge and an appropriate total effective core potential.⁶¹ The results are reported in Table 1. This strategy has been efficiently used to provide an adequate

Table 1. Magnetic Coupling Constants of the Dinuclear Model Systems (in cm^{-1}) as Predicted from Different DFT-based Methods^a

	J_{12}	J_{23}	J_{23}/J_{12}
BHHLYP	−214	−192	0.898
M06-2X	−228	−205	0.900
LC- ω PBE	−443	−399	0.901
HSEH1PBPE	−613	−566	0.923
B3LYP	−735	−682	0.928
M06	−754	−699	0.927

^aThe rightmost column reports the J_{23}/J_{12} ratios.

environment to cluster models of high critical temperature superconducting cuprates parent compounds.^{62,63} For this new model, calculated values with different functionals differ, as expected, but are all of the order of magnitude of the experimentally derived magnetic coupling constant in HAKKEJ. In these calculations, the spin density is almost completely localized on the Cu atoms, and the expectation value of the square of the total spin operator ($\langle S^2 \rangle$) is ~ 2.0 for the high spin and ~ 1.0 for the low spin broken symmetry solution as predictable. Additionally, all the coupling constants of the dinuclear units calculated with the different DFT functionals point to the fact that the antiferromagnetic interactions between the crystallographic Cu(1)–Cu(2) magnetic centers are more intense than for the Cu(2)–Cu(3) ones, indicating that $|J_{12}| > |J_{23}|$ and, more specifically, that irrespective of the functional, $J_{12}/J_{23} \sim 0.9$ (Table 1). We will come back to this important conclusion later on when discussing the results for the trinuclear complex. Here, let us advance that the $J_{12}/J_{23} \sim 0.9$ relation also holds when explicitly dealing with the whole molecular structure of HAKKEJ but substituting Cu₁ or Cu₃ by the TIP.

For the trinuclear dication, calculations were carried out for the $|\alpha\alpha\alpha\rangle$ high spin state and for the three $|\alpha\alpha\beta\rangle$, $|\alpha\beta\alpha\rangle$, and

$|\beta\alpha\alpha\rangle$ broken symmetry solutions. In all cases, the electronic ground state corresponds to the $|\alpha\beta\alpha\rangle$ broken symmetry solution, indicating a dominant antiferromagnetic character, in agreement with the experiment. Moreover, the $|\beta\alpha\alpha\rangle$ solution is always slightly more stable than the $|\alpha\alpha\beta\rangle$, which seems to indicate that $J_{12} > J_{23}$ as suggested by the results on the artificially cut dinuclear models. From the mapping procedure (eqs 16–18), it is possible to extract the three magnetic coupling constants which are reported in Table 2. From the

Table 2. Magnetic Coupling Constants of the Trinuclear HAKKEJ Compound (in cm^{-1}) as Predicted from Different DFT-based Methods^a

	J_{12}	J_{23}	J_{13}	J_{23}/J_{12}	J_{13}/J_{12}
BHHLYP	−211	−190	−0.4	0.899	0.002
M06-2X	−224	−202	−0.5	0.902	0.002
LC- ω PBE	−440	−397	−2	0.903	0.005
HSEH1PBPE	−620	−576	−6	0.929	0.010
B3LYP	−750	−700	−10	0.933	0.013
M06	−769	−716	−10	0.932	0.013

^aThe two rightmost columns report two linear independent ratios. The experimental data fitted to a single magnetic coupling constant gives $J = -379$ cm^{-1} .³²

values reported, one can conclude that $J_{12} > J_{23}$, which has implications in the hypothesis used to extract J from fitting the experimental data. The calculated values are all in the -200 to -700 cm^{-1} range, which are on the order of magnitude of the experimentally derived J value of -379 cm^{-1} . Interestingly, for a given functional, the values reported in Table 2 nicely coincide with those reported in Table 1 and extracted from the dinuclear models including a representation of the third magnetic center. Even more, the results in Table 2 can be reproduced from calculations in HAKKEJ models where each one of the Cu sites is alternatively substituted by the TIP.

Unfortunately, in spite of the coherence of the ratios of the calculated values, these results exhibit a too large dependence with the exchange–correlation functional. This is consistent with previous studies^{12–15} but at the same time precludes a more accurate prediction. Note, however, that LC- ω PBE provides the best estimate, in agreement with previous works for antiferromagnetic Cu(II) dinuclear complexes.⁶⁴ Nevertheless, this functional fails to predict the difference in the magnitude of the magnetic coupling constant in a series of ferromagnetic compounds⁶⁵ and also performs quite badly in organic diradicals with high spin ground state.⁶⁶

The exceedingly large dependence of the calculated results with respect to the choice of the exchange–correlation functional and their shortcoming in describing the ferromagnetic description represents a clear limitation of the DFT-based methods. The general trends and magnetostuctural correlations are well described, but the magnitude of the magnetic coupling constants is not. To overcome this problem, it is highly desirable to make use of methods of quantum chemistry based on accurate wave functions. However, in the present case, the magnetic coupling constants cannot be extracted from the energy difference (see Section 2) and will need to rely on effective Hamiltonian theory. In order to overcome the tedious procedure required to compute the elements of the effective Hamiltonian matrix representations, one can make use of the additional information in the two rightmost columns of Table 2 reporting the J_{23}/J_{12} and J_{13}/J_{12} ratios for the different DFT

methods. Table 2 shows that while the calculated values of the magnetic coupling constants are strongly dependent on the DFT methods used, J_{23}/J_{12} and J_{13}/J_{12} are much less dependent and, in particular, J_{23}/J_{12} is almost constant. This is for sure the reason behind the success of DFT calculations in describing magnetostructural correlations.¹¹ Consequently, one can make use of this additional information extracted from the DFT calculations to derive the magnetic coupling constants using energy differences of spin-adapted wave functions. In particular, one could use the J_{23}/J_{12} almost constant value and eqs 9 and 10 to determine the three coupling constants. The resulting set of three equations can be solved numerically, for instance, by using a Newton–Raphson method. Table 3 reports the calculated values of the three magnetic coupling constants at different levels of ab initio wave function theory.

Table 3. Magnetic Coupling Constants of the Trinuclear HAKKEJ Compound (in cm^{-1}) as Predicted from Different Wave Function-based Methods Using eqs 9 and 10 with $J_{23}/J_{12} = 0.9^a$

methods	orbital set	J_{12}	J_{23}	J_{13}
CASSCF(3,3)	SA	−35	−31	2
	SS	−35	−32	2
CASPT2	SA	−181	−163	−129
	SS	−205	−184	−92
MRMP	SA	−161	−144	−33
	SS	−192	−173	11
DDCI	Q	−223	−200	−1

^aSA, SS, and Q stand for state average, state specific, and quartet, respectively, and refer to the orbital set used to carry out each set of calculations. The experimental data fitted to a single magnetic coupling constant gives $J = -379 \text{ cm}^{-1}$.³²

The analysis of the results in Table 3 provides a number of significant conclusions and also some surprises. The CASSCF-calculated values for J_{12} and J_{23} are, not surprisingly, too small with respect to the experimental estimate, but the J_{13} value is correctly predicted to be much smaller. Moreover, the CASSCF-calculated values are only slightly sensitive to the choice of the orbital set; calculations with state average or state specific CASSCF orbital lead to almost the same set of results. These results follow the trends described in previous works for dinuclear complexes;^{5,8} the underestimation of the magnetic coupling constants being due to the lack of dynamical correlation in the CASSCF wave function. Including dynamical correlation through the CASPT2 method improves the prediction of J_{12} and J_{23} values, which are now considerably larger although still represent $\sim 50\%$ of the experimental estimate (-379 cm^{-1}) only. The dependence of the results on the orbital set used in the CASPT2 calculations is moderate and also follows the expected trends. However, the CASPT2 estimate for J_{13} appears to be exceedingly large and can only be interpreted as an artifact arising from the contracted nature of the method. This is confirmed by the MRMP calculations, which predict similar values for J_{12} and J_{23} but a much smaller J_{13} value. Note also that this latter value is largely affected by the orbitals set used to include the second order perturbation, which indicates the delicate interplay between the three magnetic coupling constants and, correspondingly, the need for an accurate estimate of the energy differences involved. This is further verified by the DDCI calculations predicting J_{12} and J_{23} values of $\sim 60\%$ of the experimental value (-379 cm^{-1}) and

an almost negligible J_{13} value, as expected from the large distance between Cu(1) and Cu(3). The calculated J_{12} and J_{23} values are still too small, but this can be attributed to the limited basis set and to the truncation of the orbital space used to carry out the DDCI calculations.

The conclusion from the set of explicitly correlated calculations coupled to the DFT results is that it is possible to obtain a reasonable, necessarily underestimated, prediction of the three magnetic coupling constants by making use of energy differences between spin states and of the DFT J_{23}/J_{12} ratio. The calculations consistently envisage that J_{12} and J_{23} are different and that J_{13} is significantly smaller than J_{12} and J_{23} but not zero. In the next section, we will discuss the implications of these results in the estimation of the coupling constants from fitting to the experimental magnetic susceptibility curves.

Before closing this part, it would be interesting to further validate the present approach by noticing that one can make use of both J_{23}/J_{12} and J_{13}/J_{12} DFT ratios in Table 2 to express the energy differences in eqs 9 and 10 as a function of J_{12} . Thus, one gets

$$E_Q - E_{D1} = A \cdot J_{12} \quad (20)$$

$$E_Q - E_{D2} = B \cdot J_{12} \quad (21)$$

allowing one to obtain the same J_{12} coupling constant from two independent equations where the A and B parameters are determined by the choice of J_{23}/J_{12} and J_{13}/J_{12} . Now one can substitute the energy differences on the left-hand side of eqs 20 and 21 with the corresponding CASSCF, CASPT2, MRMP, and DDCI numerical values. The closer the J_{12} computed from eqs 20 and 21 is, the better the description of the Heisenberg spectrum by the method of choice is. It is worth pointing out that while J_{23}/J_{12} is almost constant and equal to 0.9, J_{13}/J_{12} varies between 0.002 for M06-2X (and BHHLYP) and 0.013 for B3LYP (and M06). However, in spite of the large variation in J_{13}/J_{12} , the A and B values exhibit a small variation as reported in the caption of Table 4. Indeed, values reported in Table 4 confirm the validity of using the DFT obtained ratios to derive the magnetic coupling constants from two accurate enough energy differences. The DDCI entry in Table 4 clearly confirms this claim. Note, however, that the CASPT2 entry in Table 4 reports quite different values for J_{12} when obtained from eq 20 or 21. This seems to indicate that the different

Table 4. Calculated Values of J_{12} As Obtained from Eqs 20 and 21 with $A = -1.45$ and $B = -0.5$ (B3LYP) and $A = -1.43$ and $B = -0.48$ (M06-2X) As Obtained from Values in Table 1^a

method	orbital set	J_{12}			
		A and B from B3LYP		A and B from M06-2x	
		eq 20	eq 21	eq 20	eq 21
CASSCF	SS	−35	−31	−35	−32
	SA	−34	−29	−35	−30
CASPT2	SS	−202	−379	−205	−396
	SA	−179	−429	−181	−449
MRMP	SS	−189	−160	−192	−168
	SA	−159	−221	−162	−231
DDCI	Q	−219	−213	−222	−223

^aSA, SS, and Q stand for state average, state specific, and quartet, respectively, and refer to the orbital set used to carry out each set of calculations.

states are not equally described by the CASPT2 methods, which can be attributed to the contracted nature of the zero-order wave function. In fact, the MRMP methods predicts results which are more consistent than CASPT2 although less reliable than those predicted from DDCI

6. IMPLICATIONS FOR EXPERIMENTALLY DERIVED COUPLING CONSTANTS

The fact that all methods, DFT- and wave function-based, consistently predict different values for J_{12} and J_{23} indicates that, in this case, the assumption of symmetry does not hold. This is also clear from the calculations on the models using the corresponding dinuclear fragments as discussed above. Likewise, it also appears that the assumption of $J_{13} = 0$ may not be rigorously justified. In order to investigate the possible consequences on the values derived from fitting to the experimental magnetic susceptibility ($\chi_M T$) versus temperature curves some considerations need to be discussed. Clearly, different sets of J_{12} , J_{23} , and J_{13} values can be derived providing a statistically meaningful fit to the $\chi_M T$ versus T values obtained from the Bleaney–Bowers equation.⁶ This is surely one of the reasons behind the hypothesis in the experimental work leading to a single magnetic coupling for this system. However, the possibility to derive a set of parameters purely from first-principles-based calculations provides an unbiased way to choose one set of parameters. This strategy was successfully used⁶⁷ some years ago to derive the dominant magnetic couplings of the Li_2CuO_2 chain compounds for which different proposals were reported with up to seven parameters included in the original fitting. The simulation with the ab initio-derived parameters was in agreement with experiment and provided a physically meaningful, unbiased picture of magnetic interactions in this chain compound.

To further illustrate procedure, the following strategy is used. In the first step, the $\chi_M T$ versus T values are obtained from the Bleaney–Bowers equation⁶ assuming the calculated (DDCI or LC- ω PBE) values for J_{12} , J_{23} , and J_{13} . In the second step, a fitting procedure is used to obtain a single value for the magnetic coupling constant assuming symmetry ($J_{12} = J_{23}$) and $J_{13} = 0$. The different sets of results are reported in Figure 4,

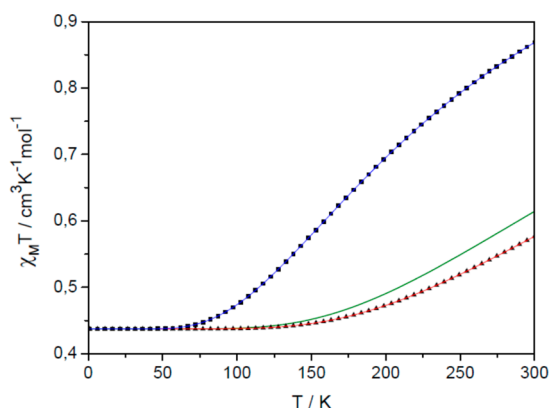


Figure 4. Molar susceptibility times temperature ($\chi_M T$) versus temperature (T) plots obtained from the Bleaney–Bowers equation using DDCI or LC- ω PBE calculated values for J_{12} , J_{23} , and J_{13} (squares and triangles, respectively). A fitting to these simulated curves employing just one magnetic coupling constant are also provide (blue and red lines, respectively). The curve fitting experimental data of ref 32 is included for comparison (green curve).

where the green line shows the $\chi_M T$ versus T values corresponding to the simulation of the original experimental data to a single J value of -379 cm^{-1} and excluding the Curie–Weiss parameter for the intermolecular interactions affecting the very low-temperature data used in ref 32. The squares correspond to the simulation of the $\chi_M T$ versus T values arising from the three DDCI magnetic coupling constants, and the triangles correspond to the simulation obtained when using the three LC- ω PBE values for the magnetic coupling constants. The blue and red curves show, respectively, the best fit of the DDCI and LC- ω PBE simulated $\chi_M T$ versus T values using a single J value. In the case of the DDCI curve, this corresponds to a J of -208.1 cm^{-1} , which is far from the experimental estimate. However, in the case of the LC- ω PBE curve a value of -418.9 cm^{-1} is obtained, which is in good agreement with experiment.

From Figure 4, it is clear that the experimental $\chi_M T$ versus T curve and the ones obtained from DDCI- or LC- ω PBE-calculated J_{12} , J_{23} and J_{13} values can be accurately fitted with just one J parameter with a value intermediate between J_{12} and J_{23} . This is not surprising since fitting procedures are known to exhibit multiple solutions. The important conclusion is, however, that without theoretical information one can at most obtain the order of magnitude of the magnetic interaction but at the cost of losing the fine details concerning the difference between J_{12} and J_{23} and the magnitude of J_{13} . However, with appropriate input from calculations, it is possible to gain a deeper insight into the underlying magnetic interactions.

The DDCI-calculated values are clearly too small, which as commented on above is not surprising and comes from the limitations in the DDCI expansion resulting in a limited description of differential electronic correlation effects. Now, for the particular systems studied in the present work, using the experimental information that the dominant magnetic coupling constants are about -400 cm^{-1} , one can come back to the DFT results in Table 2 to obtain a more accurate picture. The calculated DFT magnetic coupling constants depend strongly on the choice of the functional, but the ones predicted by the LC- ω PBE method are precisely in the range of the experimental value. Hence, one can safely take this set of results as a reasonable prediction. Clearly, taking $J_{12} = -440 \text{ cm}^{-1}$, $J_{23} = -397 \text{ cm}^{-1}$, and $J_{13} = -2 \text{ cm}^{-1}$ leads to the $\chi_M T$ versus T curve (triangles sequence, Figure 4) close to the experimental one (simulated green curve, Figure 4). We must insist on the fact that these data can be fitted with a single J value of -418.9 cm^{-1} (red curve, Figure 4), which is close enough to the experimentally reported value.

7. CONCLUSIONS

In the case of binuclear complexes, deriving magnetic coupling constants from ab initio calculations is straightforward and well established.^{2–5} However, difficulties are present when handling more complicated systems such as heterodinuclear complexes, as discussed in a recent work.²¹ The case of trinuclear complexes introduces a different type of difficulty since the number of pure spin states does not offer sufficient information to extract the different magnetic coupling constants from the corresponding energy differences and one is thus bound to use effective Hamiltonian theory,⁵ which while elegant and robust is difficult to use by nonspecialists and requires a considerable computational effort.

The existence of a larger number of broken symmetry states seems to offer a way out since the required energy differences can be written. However, in that case, one maps expectation values of the exact and HDVV Hamiltonian obtained from the different broken symmetry solutions. This is at variance of the usual mapping involving the energy of the pure spin states and the eigenvalues of the HDVV Hamiltonian. Still, the mapping involving expectation values and broken symmetry solutions is robust, and the only problem comes from the too large dependence on the calculated results with the form of the exchange–correlation potential used to compute the energy of the different broken symmetry solutions. At this point, one needs either information from experiment or from ab initio wave function-based calculations. In this work, we have shown that while the calculated magnetic coupling constants depend on the DFT method used, the ratio between the different magnetic coupling constants is almost constant. This is surely the reason behind the success of DFT in predicting magnetostructural relationships.³ This almost constant ratio between different coupling constants provides extra information to derive the magnetic coupling constants from energy differences between spin states. In this way, one would combine ab initio wave function energy differences (e.g., obtained from DDCI calculations) between the pure spin states and the DFT-derived ratio leading to a convenient approach.⁴

The three magnetic couplings of the trinuclear HAKKEJ complex constants have been obtained, and the results consistently show that the two dominant coupling constants are not equal and that the smallest one is not zero. However, the magnetic coupling constants thus obtained are smaller than the single value obtained from the experiment assuming symmetry and neglecting one of the couplings. The underestimation of the magnetic coupling constants comes from the limited inclusion of electronic correlation probably due to the necessary truncation of the orbital space.

Interestingly, the values obtained with the LC- ω PBE functional are in the range of the experimental value commented on above, which suggest that the three magnetic coupling constants derived from the broken symmetry calculations provide a reliable estimate. The values thus obtained also indicate that the two dominant coupling constants are significantly different and that the smallest one is almost negligible but not zero. This result has implications for the interpretation of the experimental $\chi_M T$ versus T curve. The simulations in the present work show that it is well possible to successfully fit the $\chi_M T$ versus T curve corresponding to a system with three different and well-defined magnetic coupling constants with a single one. The information thus obtained is just an average, and the details of the magnetic interactions are lost. Using the calculated values to guide the fitting will provide a much deeper insight in the details of the magnetic system. The strategy suggested in the present work regarding the representation of different magnetic centers by appropriate total ion potentials can be extended to more complicated systems in a quite straightforward way.

AUTHOR INFORMATION

Corresponding Author

*E-mail: francesc.illas@ub.edu.

Notes

The authors declare no competing financial interest.

ACKNOWLEDGMENTS

This work has been supported by Spanish MINECO through research grants PRI-PIBIN-2011-1028 and CTQ2012-30751 and by Generalitat de Catalunya grants 2014SGR97, XRQTC.

REFERENCES

- (1) Kahn, O. *Molecular Magnetism*; VCH: New York, 1993.
- (2) Datta, S. N.; Trindle, C. O.; Illas, F. *Theoretical and Computational Aspects of Magnetic Organic Molecules*; Imperial College Press: London, 2014.
- (3) Ciofini, I.; Daul, C. A. DFT calculations of molecular magnetic properties of coordination compounds. *Coord. Chem. Rev.* **2003**, 238–239, 187–209.
- (4) Moreira, I. de P. R.; Illas, F. A Unified View of the Theoretical Description of Magnetic Coupling in Molecular Chemistry and Solid State Physics. *Phys. Chem. Chem. Phys.* **2006**, 8, 1645–1659.
- (5) Malrieu, J. P.; Caballol, R.; Calzado, C. J.; de Graaf, C.; Guihery, N. Magnetic Interactions in Molecules and Highly Correlated Materials: Physical Content, Analytical Derivation, and Rigorous Extraction of Magnetic Hamiltonians. *Chem. Rev.* **2014**, 114, 429–492.
- (6) Bleaney, B.; Bowers, K. D. Anomalous Paramagnetism of Copper Acetate. *Proc. R. Soc. London, Ser. A* **1952**, 214, 451–465.
- (7) Miralles, J.; Castell, O.; Caballol, R.; Malrieu, J. P. Specific CI Calculation of Energy Differences: Transition Energies and Bond Energies. *Chem. Phys.* **1993**, 172, 33–43.
- (8) Graaf, C. de; Sousa, C.; Moreira, I. de P. R.; Illas, F. Multiconfigurational perturbation theory, an efficient tool to predict magnetic coupling parameters in biradicals, molecular complexes and ionic insulators. *J. Phys. Chem. A* **2001**, 105, 11371–11378.
- (9) Negodaev, I.; Queralt, N.; Caballol, R.; Graaf, C. de Theoretical Study of the Magnetic Exchange Interaction in Catena- μ -Tris-[oxalato(2-)-O-1,O-2;O-3,O-4]-Dicopper Complex with Interlocked Helical Chains. *Chem. Phys.* **2011**, 379, 109–115.
- (10) Negodaev, I.; de Graaf, C.; Caballol, R.; Lukov, V. V. On the Magnetic Coupling in Asymmetric Bridged Cu(II) Dinuclear Complexes: The Influence of Substitutions on the Carboxylato Group. *Inorg. Chim. Acta* **2011**, 375, 166–172.
- (11) Ruiz, E.; Alemany, P.; Alvarez, S.; Cano, J. Toward the Prediction of Magnetic Coupling in Molecular Systems: Hydroxo- and Alkoxo-bridged Cu(II) Binuclear Complexes. *J. Am. Chem. Soc.* **1997**, 119, 1297–1303.
- (12) Caballol, R.; Castell, O.; Illas, F.; Malrieu, J. P.; Moreira, I. de P. R. Remarks on the Proper Use of the Broken Symmetry Approach to Magnetic Coupling. *J. Phys. Chem. A* **1997**, 101, 7860–7866.
- (13) Valero, R.; Costa, R.; Moreira, I. de P. R.; Truhlar, D. G.; Illas, F. Performance of the M06 Family of Exchange–Correlation Functionals for Predicting Magnetic Coupling in Organic and Inorganic Molecules. *J. Chem. Phys.* **2008**, 128, 114103.
- (14) Rivero, P.; Moreira, I. de P. R.; Illas, F.; Scuseria, G. E. Reliability of range separated hybrids functionals in describing magnetic coupling in molecular systems. *J. Chem. Phys.* **2008**, 129, 184110.
- (15) Costa, R.; Moreira, I. de P. R.; Youngme, S.; Siri Wong, K.; Wannarit, N.; Illas, F. Toward the Design of Ferromagnetic Molecular Complexes: Magnetostructural Correlations in Ferromagnetic Triply Bridged Dinuclear Cu(II) Compounds Containing carboxylato and Hydroxo Bridges. *Inorg. Chem.* **2010**, 49, 285–294.
- (16) Calzado, C. J.; Cabrero, J.; Malrieu, J. P.; Caballol, R. Analysis of the Magnetic Coupling in Binuclear Complexes. I. Physics of the Coupling. *J. Chem. Phys.* **2002**, 116, 2728–2747.
- (17) Calzado, C. J.; Cabrero, J.; Malrieu, J. P.; Caballol, R. Analysis of the Magnetic Coupling in Binuclear Complexes. II. Derivation of Valence Effective Hamiltonians from ab initio CI and DFT Calculations. *J. Chem. Phys.* **2002**, 116, 3985–3999.
- (18) Calzado, C. J.; Angeli, C.; Taratiel, D.; Caballol, R.; Malrieu, J. P. Analysis of the Magnetic Coupling in Binuclear Systems. III. The Role of the Ligand to Metal Charge Transfer Excitations Revisited. *J. Chem. Phys.* **2009**, 131, 044327.

- (19) Neese, F. Prediction of Molecular Properties and Molecular Spectroscopy with Density Functional Theory: From Fundamental Theory to Exchange-Coupling. *Coord. Chem. Rev.* **2009**, *253*, 526–563.
- (20) Illas, F.; Moreira, I. de P. R.; de Graaf, C.; Barone, V. Magnetic Coupling in Biradicals, Binuclear Complexes and Wide Gap Insulators: A Survey of Ab Initio Wave Function and Density Functional Theory Approaches. *Theor. Chem. Acc.* **2000**, *104*, 265–272.
- (21) Costa, R.; Valero, R.; Mañeru, D. R.; Moreira, I. de P. R.; Illas, F. Spin Adapted versus Broken Symmetry Approaches in the Description of Magnetic Coupling in Heterodinuclear Complexes. *J. Chem. Theory Comput.* **2015**, *11*, 1006–1019.
- (22) Terashima, S.; Newton, G. N.; Shiga, T.; Oshio, H. Planar Trinuclear Complexes with Linear Arrays of Metal Ions. *Inorg. Chem. Front.* **2015**, *2*, 125–128.
- (23) Moreira, I. de P. R.; Suaud, N.; Guihéry, N.; Malrieu, J. P.; Caballol, R.; Boffill, J. M.; Illas, F. Derivation of spin Hamiltonians from the exact Hamiltonian: Application to systems with two unpaired electrons per magnetic site. *Phys. Rev. B: Condens. Matter Mater. Phys.* **2002**, *66*, 134430.
- (24) Mayhall, N. J.; Head-Gordon, M. Computational Quantum Chemistry for Multiple-Site Heisenberg Spin Couplings Made Simple: Still Only One Spin–Flip Required. *J. Phys. Chem. Lett.* **2015**, *6*, 1982–1988.
- (25) Noodleman, L. Valence Bond Description of Anti-Ferromagnetic Coupling in Transition-Metal Dimers. *J. Chem. Phys.* **1981**, *74*, 5737.
- (26) Noodleman, L.; Davidson, E. R. Ligand Spin Polarization and Antiferromagnetic Coupling in Transition-Metal Dimers. *Chem. Phys.* **1986**, *109*, 131.
- (27) Noodleman, L.; Peng, C. Y.; Case, D. A.; Mouesca, J. M. Orbital Interactions, Electron Delocalization and Spin Coupling in Iron-Sulfur Clusters. *Coord. Chem. Rev.* **1995**, *144*, 199.
- (28) Mouesca, J. M.; Noodleman, L.; Case, D. A. Density-Functional Calculations of Spin Coupling in $[\text{Fe}_4\text{S}_4]^{3+}$ Clusters. *Int. J. Quantum Chem.* **1995**, *56*, 95.
- (29) Sinn, E. Magnetic Exchange in Polynuclear Metal Complexes. *Coord. Chem. Rev.* **1970**, *5*, 313–347.
- (30) Martin, R. L.; Illas, F. Antiferromagnetic Exchange Interactions from Hybrid Density Functional Theory. *Phys. Rev. Lett.* **1997**, *79*, 1539–1542.
- (31) Illas, F.; Martin, R. L. Magnetic coupling in ionic solids studied by density functional theory. *J. Chem. Phys.* **1998**, *108*, 2519–2527.
- (32) Costa, R.; Garcia, A.; Ribas, J.; Mallah, T.; Journaux, Y.; Sletten, J.; Solans, X.; Rodriguez, V. Tailored Magnetic Properties in Trinuclear Copper(II) Complexes: Synthesis, Structure, and Magnetic Properties of Complexes Derived from [1,3-propanediylbis-(oxamato)]cuprate(II) ($[\text{Cu}(\text{pba})]^{2-}$). *Inorg. Chem.* **1993**, *32*, 3733–3742.
- (33) Ribas, J.; Garcia, A.; Costa, R.; Monfort, M.; Alvarez, S.; Zanchini, C.; Solans, X.; Domenech, M. V. Dinuclear Complexes of Copper(II) Derived from (1,3-Propanediylbis(Oxamato))Cuprate(II): Magneto-Structural Correlations. *Inorg. Chem.* **1991**, *30*, 841–845.
- (34) Frisch, M. J.; Trucks, G. W.; et al. *Gaussian 09*, Revision A.1; Gaussian, Inc.: Wallingford, CT, 2009.
- (35) Becke, A. D. A New Mixing of Hartree–Fock and Local Density-Functional Theories. *J. Chem. Phys.* **1993**, *98*, 1372.
- (36) Becke, A. D. Density-Functional Thermochemistry. III. The Role of Exact Exchange. *J. Chem. Phys.* **1993**, *98*, 5648–5652.
- (37) Zhao, Y.; Truhlar, D. G. A New Local Density Functional for Main-Group Thermochemistry, Transition Metal Bonding, Thermochemical Kinetics, and Noncovalent Interactions. *J. Chem. Phys.* **2006**, *125*, 194101–194118.
- (38) Zhao, Y.; Truhlar, D. G. Density Functional for Spectroscopy: No Long-Range Self-Interaction Error, Good Performance for Rydberg and Charge-Transfer States, and Better Performance on Average than B3LYP for Ground States. *J. Phys. Chem. A* **2006**, *110*, 13126–13130.
- (39) Zhao, Y.; Truhlar, D. G. The M06 Suite of Density Functionals for Main Group Thermochemistry, Thermochemical Kinetics, Non-covalent Interactions, Excited States, and Transition Elements: Two New Functionals and Systematic Testing of four M06-class Functionals and 12 other Functionals. *Theor. Chem. Acc.* **2008**, *120*, 215–241.
- (40) Heyd, J.; Scuseria, G. E.; Ernzerhof, M. Hybrid Functionals Based on a Screened Coulomb Potential. *J. Chem. Phys.* **2003**, *118*, 8207; *J. Chem. Phys.* **2006**, *124*, 219906.
- (41) Heyd, J.; Scuseria, G. E. Assessment and Validation of a Screened Coulomb Hybrid Density Functional. *J. Chem. Phys.* **2004**, *120*, 7274–7280.
- (42) Vydrov, O. A.; Scuseria, G. E. Assessment of a Long-Range Corrected Hybrid Functional. *J. Chem. Phys.* **2006**, *125*, 234109–234119.
- (43) Roos, B. O.; Taylor, P. R.; Siegbahn, P. E. M. A complete active space SCF method (CASSCF) using a density matrix formulated super-CI approach. *Chem. Phys.* **1980**, *48*, 157–173.
- (44) Miralles, J.; Castell, O.; Caballol, R.; Malrieu, J. P. Specific CI Calculation of Energy Differences: Transition Energies and Bond Energies. *Chem. Phys.* **1993**, *172*, 33–43.
- (45) Andersson, K.; Malmqvist, P.-Å.; Roos, B. O.; Sadlej, A. J.; Wolinski, K. Second-Order Perturbation Theory with a CASSCF Reference Function. *J. Phys. Chem.* **1990**, *94*, 5483–5488.
- (46) Andersson, K.; Malmqvist, P.-Å.; Roos, B. O. *J. Chem. Phys.* **1992**, *96*, 1218–1226.
- (47) Graaf, C. de; Sousa, C.; Moreira, I. de P. R.; Illas, F. Multiconfigurational Perturbation Theory: An Efficient Tool to Predict Magnetic Coupling Parameters in Biradicals, Molecular Complexes, and Ionic Insulators. *J. Phys. Chem. A* **2001**, *105*, 11371–11378.
- (48) Hirao, K. Multireference Møller–Plesset Perturbation Treatment of Potential Energy Curve of N_2 . *Int. J. Quantum Chem.* **1992**, *44*, 517–526.
- (49) Hirao, K. Multireference Møller–Plesset Method. *Chem. Phys. Lett.* **1992**, *190*, 374–380.
- (50) Hirao, K. Multireference Møller–Plesset Perturbation Theory for High-Spin Open-Shell Systems. *Chem. Phys. Lett.* **1992**, *196*, 397–403.
- (51) Hirao, K. State-Specific Multireference Møller–Plesset Perturbation Treatment for Singlet and Triplet Excited States, Ionized States and Electron Attached States of H_2O . *Chem. Phys. Lett.* **1993**, *201*, 59–66.
- (52) Aquilante, F.; de Vico, L.; Ferre, N.; Ghigo, G.; Malmqvist, P.-Å.; Pedersen, T.; Pitonak, M.; Reiher, M.; Roos, B. O.; Serrano Andres, L.; Urban, M.; Veryazov, V.; Lindh, R. Software News and Update MOLCAS 7: The Next Generation. *J. Comput. Chem.* **2010**, *31*, 224–247.
- (53) Ben Amor, N.; Maynau, D. CASDI program: Package developed at the Laboratoire de Chimie et Physique Quantiques, Université Paul Sabatier, Toulouse (France). *Chem. Phys. Lett.* **1998**, *286*, 211.
- (54) Schmidt, M. W.; Baldridge, K. K.; Boatz, J. A.; Elbert, S. T.; Gordon, M. S.; Jensen, J. H.; Koseki, N.; Matsunaga, K.; Nguyen, A.; Su, S.; Windus, T. L.; Dupuis, M. J.; Montgomery, A. General Atomic and Molecular Electronic Structure System. *J. Comput. Chem.* **1993**, *14*, 1347–1363.
- (55) Gordon, M. S.; Schmidt, M. W. Advances in Electronic Structure Theory: GAMESS a Decade Later. In *Theory and Applications of Computational Chemistry: the First Forty Years*; Dykstra, C. E., Frenking, G., Kim, K. S., Scuseria, G. E., Eds.; Elsevier: Amsterdam, 2005; pp 1167–1189.
- (56) Hehre, W. J.; Ditchfield, R.; Pople, J. A. Self-Consistent Molecular Orbital Methods. XII. Further Extensions of Gaussian-Type Basis Sets for Use in Molecular Orbital Studies of Organic Molecules. *J. Chem. Phys.* **1972**, *56*, 2257–2261.
- (57) Ditchfield, R.; Hehre, W. J.; Pople, J. A. Self-Consistent Molecular-Orbital Methods. IX. An Extended Gaussian-Type Basis for Molecular-Orbital Studies of Organic Molecules. *J. Chem. Phys.* **1971**, *54*, 724–728.
- (58) Hay, P. J.; Wadt, W. R. Ab Initio Effective Core Potentials for Molecular Calculations. Potentials for the Transition Metal Atoms Sc to Hg. *J. Chem. Phys.* **1985**, *82*, 270–283.

- (59) Hay, P. J.; Wadt, W. R. Ab Initio Effective Core Potentials for Molecular Calculations. Potentials for Main Group Elements Na to Bi. *J. Chem. Phys.* **1985**, *82*, 284–298.
- (60) Hay, P. J.; Wadt, W. R. Ab Initio Effective Core Potentials for Molecular Calculations. Potentials for K to Au Including the Outermost Core Orbitals. *J. Chem. Phys.* **1985**, *82*, 299–310.
- (61) Martin, R. L. Cluster studies of La_2CuO_4 : A mapping onto the Pariser–Parr–Pople (PPP) model. *J. Chem. Phys.* **1993**, *98*, 8691–8697.
- (62) Muñoz, D.; Moreira, I. de P. R.; Illas, F. Accurate prediction of large antiferromagnetic interactions in High- T_c $\text{HgBa}_2\text{Ca}_{n-1}\text{Cu}_n\text{O}_{2n+2+\delta}$ ($n=2,3$) superconductor parent compounds. *Phys. Rev. Lett.* **2000**, *84*, 1579–1582.
- (63) Moreira, I. de P. R.; Calzado, C. J.; Malrieu, J. P.; Illas, F. Four-body spin terms in High- T_c cuprates. *Phys. Rev. Lett.* **2006**, *96*, 087003.
- (64) Wannarit, N.; Siri Wong, K.; Chaichit, N.; Youngme, S.; Costa, R.; Moreira, I. de P. R.; Illas, F. A New Series of Triply-Bridged Dinuclear Cu(II) Compounds: Synthesis, Crystal Structure, Magnetic Properties and Theoretical Study. *Inorg. Chem.* **2011**, *50*, 10648–10659.
- (65) Wannarit, N.; Pakawatchai, Ch.; Mutikainen, I.; Costa, R.; Moreira, I. de P. R.; Youngme, S.; Illas, F. Hetero Triply-Bridged Dinuclear Copper(II) Compounds with Ferromagnetic Coupling: A Challenge for Current Density Functionals. *Phys. Chem. Chem. Phys.* **2013**, *15*, 1966–1975.
- (66) Reta Mañeru, D.; Pal, A. K.; Moreira, I. de P. R.; Datta, S. N.; Illas, F. The Triplet-Singlet Gap in the m-Xylylene Radical: a not so Simple One. *J. Chem. Theory Comput.* **2014**, *10*, 335–345.
- (67) de Graaf, C.; Moreira, I. de P. R.; Illas, F.; Iglesias, O.; Labarta. The magnetic structure of Li_2CuO_2 : from ab initio calculations to macroscopic simulations. *A. Phys. Rev. B: Condens. Matter Mater. Phys.* **2002**, *66*, 014448.